Med Biol Eng Comput (2013) 51:581–591
DOI 10.1007/s11517-012-1028-z

ORIGINAL ARTICLE

Testing pattern synchronization in coupled systems through different entropy-based measures

Peng Li · Chengyu Liu · Xinpei Wang · Liping Li · Lei Yang · Yongcai Chen · Changchun Liu

Received: 11 July 2012 / Accepted: 22 December 2012 / Published online: 22 January 2013

Abstract Pattern synchronization (PS) can capture one aspect of the dynamic interactions between bivariate physiological systems. It can be tested by several entropy-based measures, e.g., cross sample entropy (X-SampEn), cross fuzzy entropy (X-FuzzyEn), multivariate multiscale entropy (MMSE), etc. A comprehensive comparison on their distinguishability is currently missing. Besides, they are highly dependent on several pre-defined parameters, the threshold value r in particular. Thus, their consistency also needs further elucidation. Based on the well-accepted assumption that a tight coupling necessarily leads to a high PS, we performed a couple of evaluations over several simulated coupled models in this study. All measures were compared to each other with respect to their consistency and distinguishability, which were quantified by two pre-defined criteria—degree of crossing (DoC) and degree of monotonicity (DoM). Results indicated that X-SampEn and X-FuzzyEn could only work well over coupled stochastic systems with meticulously selected r. It is thus not recommended to apply them to the intrinsic complex physiological systems. However, MMSE was suitable for both, indicating by relatively higher DoC and DoM values. Final analysis on the cardiorespiratory coupling validated our results.

P. Li · C. Liu · X. Wang · L. Yang · Y. Chen · C. Liu (✉)
School of Control Science and Engineering, Shandong University, 17923 Jingshi Road, Jinan 250061, People's Republic of China
e-mail: lskyp@mail.sdu.edu.cn; changchunliu@sdu.edu.cn

L. Li
Biomedical Engineering, College of Science and Technology, Shandong University of Traditional Chinese Medicine, Daxue Road, Jinan 250355, People's Republic of China

Keywords Consistency and distinguishability · Cross sample entropy (X-SampEn) · Cross fuzzy entropy (X-FuzzyEn) · Multivariate multiscale entropy (MMSE) · Pattern synchronization

1 Introduction

Physiological variability in blood pressure, heart rate, respiration rate, etc., can shed light onto the activities of the underlying control mechanisms [30]. However, the overwhelming proportion of the cardiorespiratory system is nonlinear, and any subtle change should be vital clinical signs for physiological or pathological transitions, which can however hardly be appreciated by conventional approaches. Researchers have benefited from the development of chaos theory and many efforts have already been made to evaluate the physiological relevance [11]. Entropy, one important measure from chaos theory, has been confirmed to be able to unveil valuable information hiding in the nonlinear complicated structures of physiological signals [1, 2, 7, 9, 13, 14, 23, 25, 29, 31–33]. Entropy evaluates the predictability or complexity for univariate signals [7, 9, 23, 25] and cross-predictability or synchronization, which is well accepted as pattern synchronization (PS) [14, 29, 31, 32], for multivariate series (mostly bivariate series). PS has been showed as a helpful tool for characterizing non-linearity of neural mechanisms underlying cardiovascular control [33] or understanding the interregional functional connectivity across the brain [14, 29, 31, 32].

Cross approximate entropy (X-ApEn) [23], cross sample entropy (X-SampEn) [25, 29, 33] and cross fuzzy entropy (X-FuzzyEn) [31, 32] can be used for testing PS. In addition, the most recently developed multivariate multiscale entropy (MMSE) [1, 2] has been proved to be catered for

direct analysis for multichannel interdependence over multiple scales, which also has a potential for evaluating PS. The above measures rely on the pattern similarity between or within different channels of bivariate series under investigation. However, a comprehensive comparison on their capability to distinguish among systems with different degrees of PS is currently missing to the best of our knowledge, which thus requires further elucidation.

Besides, their calculation requires a priori determination of three unknown parameters—embedding dimension m, threshold value r, and gradient parameter n. It is usually set at 2 or 3 for m no matter how it is chosen (empirically [23] or by estimation [16]). The parameter n determines the gradient of the boundary of the fuzzy membership function in X-FuzzyEn [31, 32]. It is usually set as 1 or 2 which has slight influence. It is r that affects the results most and thus requires meticulous selection [6, 8, 19, 21, 23]. Although several approaches based on empirical selection [23] or automatic estimation [8, 21] have already been well studied, they are however failed when applied to physiological signals [19]. It seems that to apply a less r-dependent measure is more feasible than to develop procedures for its automatic estimation. Thus, the consistency with its variation also needs serious consideration.

Altogether, the uncertainty in their distinguishability and consistency drives the desire for more rigorous studies. For experimental data the underlying synchronization information is usually unknown in advance, it is thus difficult to validate different measures through them. Simulation models with their underlying dynamics completely known are competent instead. Based on the assumption that an increase of coupling strength c necessarily leads to an increase of synchronization [4, 17, 27, 28, 31], we employed two linearly coupled stochastic systems (coupled broadband noise model [4, 31] and coupled MIX(p) processes) and two nonlinearly coupled chaotic systems (coupled Hénon maps [17, 28] and coupled Rössler systems [17, 27, 31]) for our evaluation. Herein, the threshold value r could be finely tuned for assessing the consistency, and ditto the coupling strength c for distinguishability. X-SampEn, X-FuzzyEn and MMSE were rigorously compared with their performances quantified by two predefined criteria, while X-ApEn was excluded because it is biased and lacks relative consistency [25, 31]. Finally to demonstrate their performances on real physiological signals, the PS in cardiorespiratory coupling was analyzed.

2 Methods

2.1 Brief descriptions of the tested PS measures

Brief descriptions of X-SampEn, X-FuzzyEn and MMSE are summarized in table 1.

2.2 Simulation models

2.2.1 Coupled broadband noise model (M1)

This coupled system was generated by mixing the common noise n_1 with two independent white noises n_2, n_3 [4, 31],

$$\begin{aligned} x &= cn_1 + (1-c)n_2 \\ y &= cn_1 + (1-c)n_3 \end{aligned} \tag{1}$$

where c varied from 0 to 0.7 in steps of 0.1.

To eliminate random factors, for each value of c, we generated 20 realizations, and the means of the corresponding 20 X-SampEn, X-FuzzyEn and MMSE results were used as the final values. Same procedures were implemented for 20 times.

2.2.2 Coupled MIX(p) processes (M2)

The MIX(p) process is a sinusoid signal of N points, where $N \times p$ (p is the probability parameter whose value is between 0 and 1) random chosen points are replaced with random noise. The details on MIX(p) are summarized in [23]. The coupled MIX(p) processes were generated by mixing one MIX(p) process with two others so as to simulate real world systems which contain large proportions of low-frequency trend,

$$\begin{aligned} x &= c\mathrm{MIX}(p_1) + (1-c)\mathrm{MIX}(p_2) \\ y &= c\mathrm{MIX}(p_1) + (1-c)\mathrm{MIX}(p_3) \end{aligned} \tag{2}$$

where c also varied from 0 to 0.7 in steps of 0.1, the probability parameters p_1, p_2 and p_3 were chosen as 0.3, 0.5 and 0.7, respectively.

Also, similar procedures were performed as in M1 to eliminate random factors.

2.2.3 Coupled Hénon maps (M3)

Mathematically, the coupled Hénon maps can be generated by the following iterations [17]:

$$\begin{aligned} x_{1,n+1} &= 1.4 - x_{1,n}^2 + b_x x_{2,n} \\ x_{2,n+1} &= x_{1,n} \\ y_{1,n+1} &= 1.4 - (cx_{1,n}y_{1,n} + (1-c)y_{1,n}^2) + b_y y_{2,n} \\ y_{2,n+1} &= y_{1,n} \end{aligned} \tag{3}$$

where we took $b_x = b_y = 0.3$ to yield identical systems and c varied from 0 to 0.8 incrementing by 0.1. The corresponding trajectories of the two oscillators can be found in [17] when c varied.

For each value of c, totally 60,000 points were firstly obtained with n iterating from 1 to 60,000. The last 50,000 points were used for the calculation. Ten pairs of episodes

Table 1 Brief descriptions of three pattern synchronization measures

X-SampEn [25]	X-FuzzyEn [31, 32]	MMSE [1, 2]
For two normalized sequences $\{u(i): 1 \le i \le N\}$ and $\{v(i): 1 \le i \le N\}$, form vector sequences: $X_i^m = \{u(i), u(i+1), \cdots, u(i+m-1)\}$ $Y_j^m = \{v(j), v(j+1), \cdots, v(j+m-1)\}$ $1 \le i, j \le N-m+1$	For two normalized sequences $\{u(i): 1 \le i \le N\}$ and $\{v(i): 1 \le i \le N\}$, form vector sequences: $X_i^m = \{u(i), u(i+1), \cdots, u(i+m-1)\} - \bar{u}(i)$ $Y_j^m = \{v(j), v(j+1), \cdots, v(j+m-1)\} - \bar{v}(j)$, $1 \le i, j \le N-m+1$, here X_i^m and Y_j^m represent m consecutive u and v values, with the local average $\bar{u}(i)$ and $\bar{v}(j)$ of the corresponding m values removed from each element	For p-variate normalized sequences $\left\{ y_{k,j} : \begin{matrix} k = 1, 2, \cdots, p \\ j = 1, 2, \cdots, N \end{matrix} \right\}$ and a scale factor ε $(1 \le \varepsilon \le E)$, coarse grain each series by $x_{k,i}^{\varepsilon} = \frac{1}{\varepsilon} \sum_{i=(j-1)\varepsilon+1}^{j\varepsilon} y_{k,j}$, $1 \le j \le \lfloor \frac{N}{\varepsilon} \rfloor$. Form $X_m^{\varepsilon}(i) = \{x_{1,i}^{\varepsilon}, x_{1,i+\tau_1}^{\varepsilon}, \cdots, x_{1,i+(m_1-1)\tau_1}^{\varepsilon}, x_{2,i}^{\varepsilon}, x_{2,i+\tau_2}^{\varepsilon}, \cdots, x_{2,i+(m_2-1)\tau_2}^{\varepsilon}, \cdots, x_{p,i}^{\varepsilon}, x_{p,i+\tau_p}^{\varepsilon}, \cdots, x_{p,i+(m_p-1)\tau_p}^{\varepsilon}\} = \{z_i^{\varepsilon}, z_{i+1}^{\varepsilon}, \cdots, z_{i+m-1}^{\varepsilon}\}$ for each ε, where $\mathbf{M} = \{m_1, m_2, \cdots, m_p\}$and $\boldsymbol{\tau} = \{\tau_1, \tau_2, \cdots, \tau_p\}$ is the embedding vector and the time lag vector, respectively, $m = \sum_{k=1}^{p} m_k$, $i = 1, 2, \cdots, N^{\varepsilon} - n$, $n = \max\{\mathbf{M}\} \times \max\{\boldsymbol{\tau}\}$ and $N^{\varepsilon} = \lfloor \frac{N}{\varepsilon} \rfloor$ which is the sequence length at scale ε. The distance between two vectors is defined as: $d\{X_m^{\varepsilon}(i), X_m^{\varepsilon}(j)\} = \max_{l=1}^{m} \{z_{i+l-1}^{\varepsilon}, z_{j+l-1}^{\varepsilon}\}$
The distance between two vectors is defined as: $d_{i,j}^m = d[X_i^m, Y_j^m] = \max_{k=0}^{m-1} \lvert u(i+k) - v(j+k) \rvert$	Define the distance between two vectors as: $d_{i,j}^m = d[X_i^m, Y_j^m] = \max_{k=0}^{m-1} \lvert u(i+k) - \bar{u}(i) - (v(j+k) - \bar{v}(j)) \rvert$	
Denote $B_i^m(r)$ the average number of j that $d_{i,j}^m \le r$ and $A_i^m(r)$ that $d_{i,j}^{m+1} \le r$ for $1 \le j \le N-m$	Define $B_i^m(r) = \sum_{j=1}^{N-m} \mu(d_{i,j}^m, n, r)/(N-m)$ and $A_i^m(r) = \sum_{j=1}^{N-m} \mu(d_{i,j}^{m+1}, n, r)/(N-m)$, where μ is the fuzzy membership function	Denote $B_i^{\varepsilon,m}(r)$ the average number of j that $d[X_m^{\varepsilon}(i), X_m^{\varepsilon}(j)] \le r, j \ne i$. Extend the dimensionality of the embedding vector from m_k to $m_k + 1$ and thus $p \times (N^{\varepsilon} - n)$ vectors[a] $X_{m+1}^{\varepsilon}(i)$ are obtained and calculate $B_i^{\varepsilon,m+1}(r)$ as the average number of j that $d[X_{m+1}^{\varepsilon}(i), X_{m+1}^{\varepsilon}(j)] \le r, j \ne i$. Then MMSE is defined by[b]: $\mathrm{MMSE}(\mathbf{M}, \boldsymbol{\tau}, r, \varepsilon) = -\ln\left(\left(\frac{1}{p(N^{\varepsilon}-n)} \sum_{i=1}^{p(N^{\varepsilon}-n)} B_i^{\varepsilon,m+1}(r) \right) / \left(\frac{1}{N^{\varepsilon}-n} \sum_{i=1}^{N^{\varepsilon}-n} B_i^{\varepsilon,m}(r) \right) \right)$
Then X-SampEn is defined by $\mathrm{X-SampEn}(m, r) = -\ln\left(\sum_{i=1}^{N-m} A_i^m(r) / \sum_{i=1}^{N-m} B_i^m(r) \right)$	Then X-FuzzyEn is defined by $\mathrm{X-FuzzyEn}(m, n, r) = -\ln\left(\sum_{i=1}^{N-m} A_i^m(r) / \sum_{i=1}^{N-m} B_i^m(r) \right)$	

[a] This can be performed in p different ways, as from a space with $\mathbf{M} = [m_1, m_2, \cdots, m_k, \cdots, m_p]$, the system can evolve to any space for which the embedding vector is $[m_1, m_2, \cdots, m_{k+1}, \cdots, m_p], k = 1, 2, \cdots, p$

[b] Note that the result of MMSE is a vector whose length is determined by the number of ε

with the length 500 were selected randomly with no overlap from the last 50,000 points and the means of X-SampEn and X-FuzzyEn results of the ten pairs were used as the final values. The mean of ten MMSE results calculated for every 5,000 points from the last 50,000 points was used as the MMSE value.

2.2.4 Coupled Rössler systems (M4)

We used the unidirectional drive-response coupled Rössler oscillators whose motion equations read:

$$\begin{aligned}
\dot{x}_1 &= -(x_2 + x_3) \\
\dot{x}_2 &= x_1 + 0.2x_2 \\
\dot{x}_3 &= 0.2 + x_3(x_1 - 5.7) \\
\dot{y}_1 &= -(y_2 + y_3) - c(y_1 - x_1) \\
\dot{y}_2 &= y_1 + 0.2y_2 \\
\dot{y}_3 &= 0.2 + y_3(y_1 - 5.7)
\end{aligned} \tag{4}$$

The equations were integrated using Runge–Kutta 4th order with a step size of 0.05 and a sampling interval of 0.3. It has already been illustrated in [27] that the trajectories of the two oscillators would be identically synchronized when $c = 0.2$. Thus, we varied c from 0 to 0.2 in steps of 0.02. The second components x_2 and y_2 were used for the calculation, which shared the same procedure as in M3.

2.3 Criteria for comparison

For all realizations from M1 to M4 with different coupling strengths, each PS measure was estimated with r varying from 0.1 to 0.8 in steps of 0.02 (all series were first normalized by its SD as described in Table 1; hence it is unnecessary of r to be multiplied by SD). The scale factor ε of MMSE was selected from 1 to 10 incrementing by 1. Thus, it resulted in a 2D-matrix for X-SampEn and X-FuzzyEn with two parameters—c and r; for MMSE, a 3D-matrix was obtained whose 3rd dimension was ε. In addition, the length of all sequences was 500 for X-SampEn and X-FuzzyEn which is sufficient for accurate results, but 5,000 for MMSE so as to guarantee that the highest scale factor ($\varepsilon = 10$) had 500 data points [1, 2]. We fixed $m = 2$ and $n = 2$ in X-SampEn and X-FuzzyEn, and $\mathbf{M} = [2, 2], \boldsymbol{\tau} = [1, 1]$ in MMSE for all calculations [1, 2, 7, 23].

Theoretically, the projection on entropy values z versus r plane when $c = c_1$ will not cross over that when $c = c_2$. Thus, their differences calculated in a point-by-point manner will have the same sign (all are greater or smaller than zero); otherwise, part of them is greater than zero and part smaller or equals to zero. We thus defined the degree of crossing (DoC),

$$\mathrm{DoC}(\varepsilon) = 1 - \frac{2}{n_c(n_c - 1)} \sum_{i=1}^{n_c - 1} \sum_{j=i+1}^{n_c} \mathrm{f}(\mathbf{z}_{i,\varepsilon}, \mathbf{z}_{j,\varepsilon}) \tag{5}$$

where $\mathbf{z}_{i,\varepsilon}$ and $\mathbf{z}_{j,\varepsilon}$ are both vectors whose lengths equal to the number of different values of r, and f is a function of two vectors which returns 0 if the differences of the two vectors have the same sign and 1 otherwise, $\varepsilon = \begin{cases} 1 & \text{for X-SampEn, X-FuzzyEn} \\ 1, 2, \cdots, 10 & \text{for MMSE} \end{cases}$, n_c is the number of different values of c. The values of DoC varies from 0 to 1 and a larger DoC value indicates a better consistency (hence with the variation of r, PS measures of any two systems will hardly switch, e.g., the result shows that the PS between $\{x, y\}$ pair is stronger than $\{m, n\}$ pair when $r = r_1$, there hardly exists an r_2 showing the PS between $\{m, n\}$ pair is stronger than $\{x, y\}$ pair).

It is believed that the similarity of the pattern architecture of the two coupled systems increases with the increase of c. Therefore, monotonously decreased X-SampEn and X-FuzzyEn series and a monotonously increased MMSE series with the increase of c will be obtained.[1] Basically, for a monotonously decreased series $e_i (i = 1, 2, \cdots, N)$, given $\forall j, 1 \le j \le N$, $\exists e_i \ge e_j$ for all $i \le j$; for a monotonously increased series $e_i (i = 1, 2, \cdots, N)$, given $\forall j, 1 \le j \le N$, $\exists e_i \le e_j$ for all $i \le j$. Thus we defined the degree of monotonicity (DoM) [17, 31].

$$\mathrm{DoM}(k, \varepsilon) = \frac{2}{n_c(n_c - 1)} \sum_{i=1}^{n_c - 1} \sum_{j=i+1}^{n_c} \mathrm{sign}((z_{i,k,\varepsilon} - z_{j,k,\varepsilon}) \times d) \tag{6}$$

where $k = 1, 2, \cdots, n_r$, n_r is the number of different values of r, $d = \begin{cases} 1 & \text{for X-SampEn, X-FuzzyEn} \\ -1 & \text{for MMSE} \end{cases}$., ε and n_c share the same meaning as in (5). For each value of r, a DoM is obtained which will attain 1 if the projection on z versus c plane strictly monotonously increases (for MMSE) or decreases (for X-SampEn and X-FuzzyEn) and -1 otherwise.

Means and SDs for DoC and DoM values were obtained from all 20 realizations of M1 and M2, while for M3 and M4 only means of them attained.

3 Results

We would like to explain first that it seems difficult to show our results for MMSE in one Cartesian coordinate system,

[1] With the increase of c, similar patterns are prone to occur. Thus the cross-predictability increases; hence X-SampEn and X-FuzzyEn decreases. However, an increase in c leads to an increase in long-range correlations both within- and between- channels which is consequently leads to an increase of MMSE.

since they were all represented by a 3D-matrix. For an intuitive description, we sliced all 3D-matrix by one parameter (ε) and a number of 2D-slices returned. Since the values might vary slightly and these slices were too close to each other, we plotted parts of them for illustration. Besides, to show how X-SampEn and X-FuzzyEn varied with different values of r, we plotted their projections (measures versus r, also part of them) in addition to the original plots. However, it also seems hard to show how MMSE at all scales varied with different values of r by the projections because in this case, we had to project the MMSE at each scale; hence a number of plots would be obtained. We did not have enough pages to show them. The results of the pre-defined criteria were showed instead. However, it should be noted that although we just plotted parts of the results for illustration, it did not mean that our results would be less illustrative. Actually, the occurrence of just one crossing on measure versus r plane would mean that it is less consistent; also, low distinguishability would be resulted if it is less monotonous of measure versus c. In addition, the pre-defined criteria were plotted using all the results, whether it was showed or not, which would be sufficient to make conclusions.

3.1 Dependence on the threshold value r

For M1, all measures decrease with the increase of r (Fig. 1a–c). The curve of X-SampEn when $c = 0.1$ crosses over that when $c = 0.2$ at about $r = 0.17 \sim 0.18$ (Fig. 1d), while no crossing-over occurs regarding X-FuzzyEn when r varies from 0.16 to 0.25 (Fig. 1e). Figure 1f summarizes their DoC values. X-FuzzyEn and MMSE at large scales ($\varepsilon \geq 5$) attain the highest DoC values. For MMSE at small scales ($\varepsilon = 1, 2$), DoC is nearly 0. And for X-SampEn and MMSE at medium scales ($\varepsilon = 3, 4$), reasonable values for DoC are obtained.

For M2, it is similar to M1 that all measures decrease with the increase of r (Fig. 2a–c). Again crossing-over occurs for X-SampEn (Fig. 2d, also at about $r = 0.17 \sim 0.18$). For X-FuzzyEn, the projections are too close to distinguish them from each other (Fig. 2e). X-SampEn, X-FuzzyEn and MMSE at very small and very large scales ($\varepsilon = 1, 9, 10$) all attain much smaller DoC values. For MMSE at medium scales ($\varepsilon = 2, 3, \cdots, 8$), their values are rather higher (Fig. 2f).

For M3 and M4, differences are observed except that all measures decrease with the increase of r (Figs. 3a–c, 4a–c).

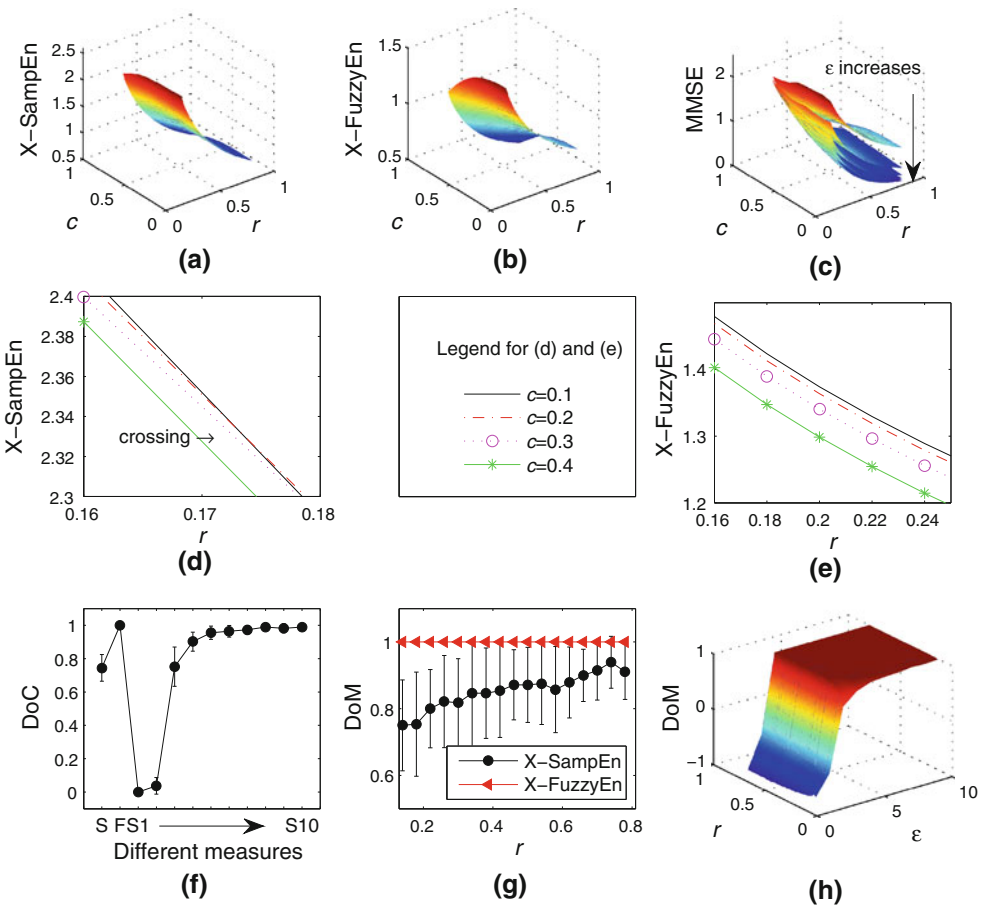

Fig. 1 Simulation results for coupled broadband noise model (M1). **a** A 3D-plot of [r, c, X-SampEn]. **b** A 3D-plot of [r, c, X-FuzzyEn]. **c** A sliced-3D-plot of [r, c, MMSE]. **d** The projection of X-SampEn versus r. **e** The projection of X-FuzzyEn versus r. **f** DoC values of X-SampEn, X-FuzzyEn and MMSE. **g** DoM values of X-SampEn and X-FuzzyEn. **h** DoM values of MMSE. X-SampEn (S), X-FuzzyEn (F) and MMSE of all 10 scales (S1 → S10) are shown from left to right in (**f**). The *curves* are plotted every other point in (**g**). The *curves* represent an average of 20 trials and *error bars* the standard deviation (SD) in (**f**) and (**g**)

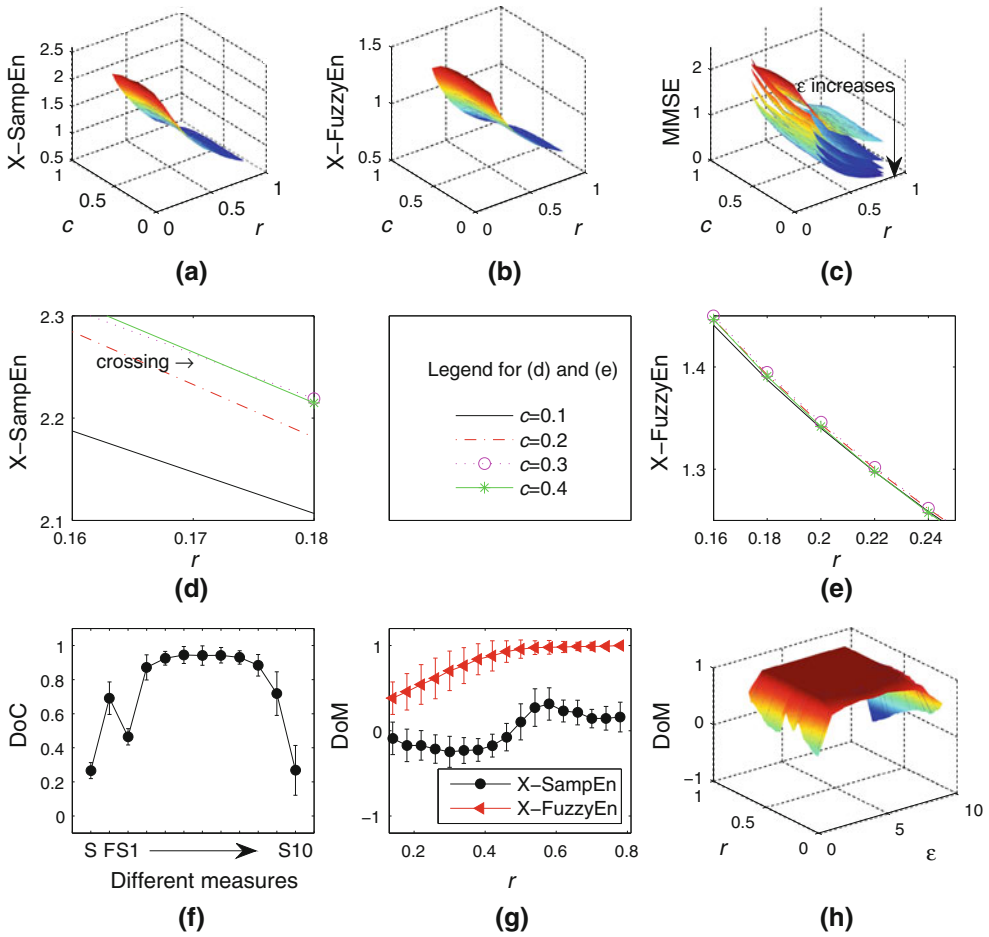

Fig. 2 Simulation results for coupled MIX(p) processes (M2). **a** A 3D-plot of [r, c, X-SampEn]. **b** A 3D-plot of [r, c, X-FuzzyEn]. **c** A sliced-3D-plot of [r, c, MMSE]. **d** The projection of X-SampEn versus r. **e** The projection of X-FuzzyEn versus r. **f** DoC values of X-SampEn, X-FuzzyEn and MMSE. **g** DoM values of X-SampEn and X-FuzzyEn. **h** DoM values of MMSE. X-SampEn (S), X-FuzzyEn (F) and MMSE of all 10 scales (S1 → S10) are shown from left to right in (**f**). The *curves* are plotted every other point in (**g**). The *curves* represent an average of 20 trials and *error bars* the standard deviation (SD) in (**f**) and (**g**)

No crossing-over occurs for X-SampEn with r from 0.15 to 0.25 (Figs. 3d, 4d), but their DoC values are all relatively small (Fig. 3f, which means crossing-over occurs at higher values of r). For X-FuzzyEn, the results either cross over each other (Fig. 3e) or are too close (Fig. 4e). Also their DoC values are all too small. However, MMSE at all scales have rather higher DoC values (Figs. 3f, 4f).

3.2 Dependence on the coupling strength c

For M1, X-SampEn decreases slightly with the increase of c when r is small and the decreasing trend is more obvious when r is larger (Fig. 1a). Similar behavior can be found for X-FuzzyEn (Fig. 1b), but the trend is more clear even for smaller r. MMSE at larger scales increases clearly with the increase of c (Fig. 1c). To evaluate their monotonicity quantitatively, the DoM values are summarized in Fig. 1g, h. They are nearly 1 at almost all values of r for X-FuzzyEn and MMSE at larger scales ($\varepsilon \geq 4$). X-SampEn and MMSE at medium scales ($\varepsilon = 3$) have reasonable DoM values but X-SampEn has significant fluctuations in different trials. MMSE at smaller scales ($\varepsilon = 1, 2$) attains negative DoM values.

For M2, a slight ceiling effect on the low values of the coupling strength can be observed for X-SampEn and X-FuzzyEn, where they both increase first and then decrease with the increase of c (Fig. 2a, b). The effect is less obvious for X-FuzzyEn at larger r. The behavior of MMSE is similar to that of M1 (Fig. 2c). For quantitative evaluation (Fig. 2g, h), the DoM values attains nearly 1 for X-FuzzyEn with large r values ($r \geq 0.5$) and MMSE at medium scales ($\varepsilon = 2, 3, \cdots, 7$), while for X-SampEn, part of them are positive but rather small and part negative when different r is selected. Also, significant fluctuations in different trials are showed.

A severe ceiling effect is observed for both X-SampEn and X-FuzzyEn regarding M3 (Fig. 3a, b), especially when smaller values of r are used, while the results for MMSE

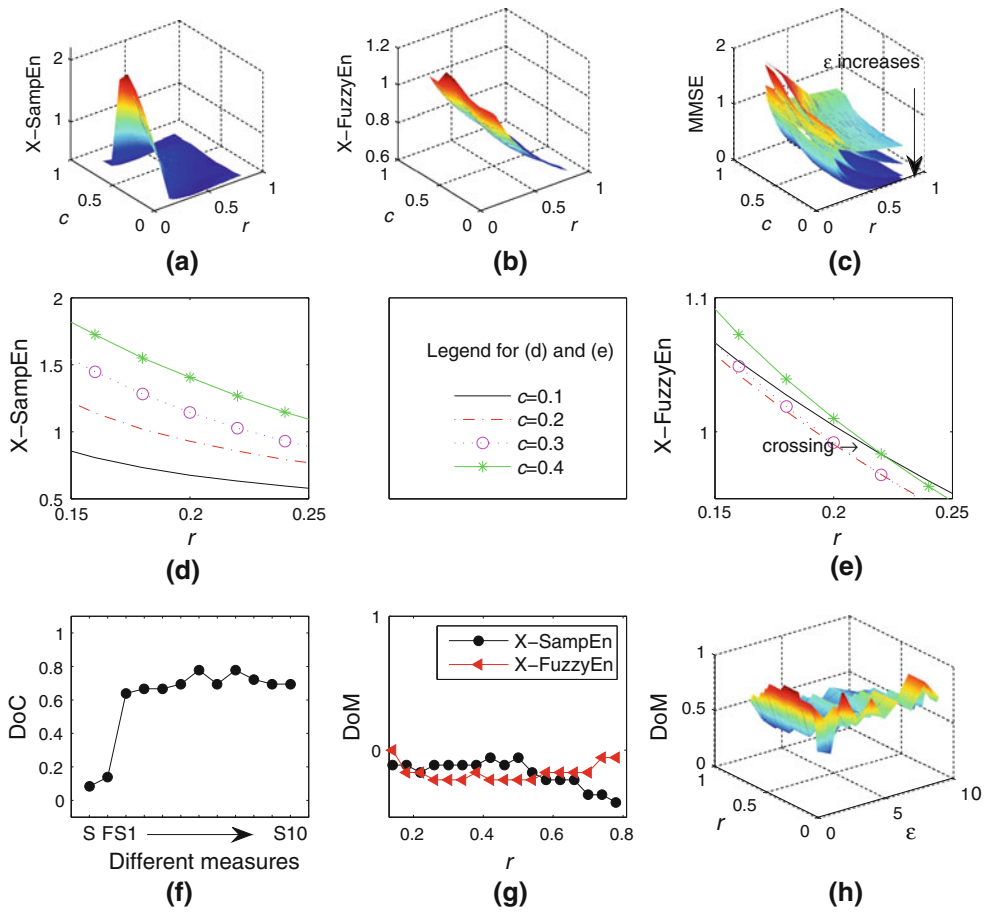

Fig. 3 Simulation results for coupled Hénon maps (M3). **a** A 3D-plot of [*r*, *c*, X-SampEn]. **b** A 3D-plot of [*r*, *c*, X-FuzzyEn]. **c** A sliced-3D-plot of [*r*, *c*, MMSE]. **d** The projection of X-SampEn versus *r*. **e** The projection of X-FuzzyEn versus *r*. **f** DoC values of X-SampEn, X-FuzzyEn and MMSE. **g** DoM values of X-SampEn and X-FuzzyEn. **h** DoM values of MMSE. X-SampEn (S), X-FuzzyEn (F) and MMSE of all 10 scales (S1 → S10) are shown from left to right in (**f**). The *curves* are plotted every other point in (**g**)

are rather monotonous (Fig. 3c). Subsequently, the DoM values for X-SampEn and X-FuzzyEn are all very small and even negative. In contrast, MMSE attains relatively reasonable DoM values.

The variation tendency of the three measures for M4 is not very obvious (Fig. 4a–c). But the quantitative results can be easily read from Fig. 4g, h. When r is small ($r \leq 0.2$) or is large enough ($r \geq 0.6$), X-SampEn attains larger DoM values, while for X-SampEn with a relatively wide medium range of r and X-FuzzyEn, the DoM values are too small. For MMSE, the DoM values are nearly 1 with almost all values of r.

3.3 Application to cardiorespiratory coupling analysis

It seems from the above results that MMSE is relatively less r-dependent. For X-SampEn and X-FuzzyEn, it also seems difficult to make conclusions about how to choose it. The only workable means is probably to choose the values which most reliably yield valuable information (a retrospective analysis, valuable information could be e.g., information useful for separating purposes, etc.).

To demonstrate the validity to physiological systems, we compared their performances on the analysis of cardiorespiratory coupling (CRC). It is believed that there are transitions in CRC with the changes of physiological states (e.g., healthy aging) [5]. Using a subset (10 healthy young and 10 healthy old with 7 women and 3 men in each group) from the FANTASIA database [12, 15], a PS decrease was also observed by MMSE analysis [1]. We would like to use another subset (also 10 healthy young and 10 healthy old but with 5 women and 5 men in each group; ECG and respiration signals were sampled at 250 Hz and lasted for 2 h) to compare the performances. Because almost all values for r worked well for MMSE according to the above simulations, we simply chose $r = 0.4$. We chose $r = 0.2$ for X-SampEn and X-FuzzyEn based on a retrospective analysis. The RRI series

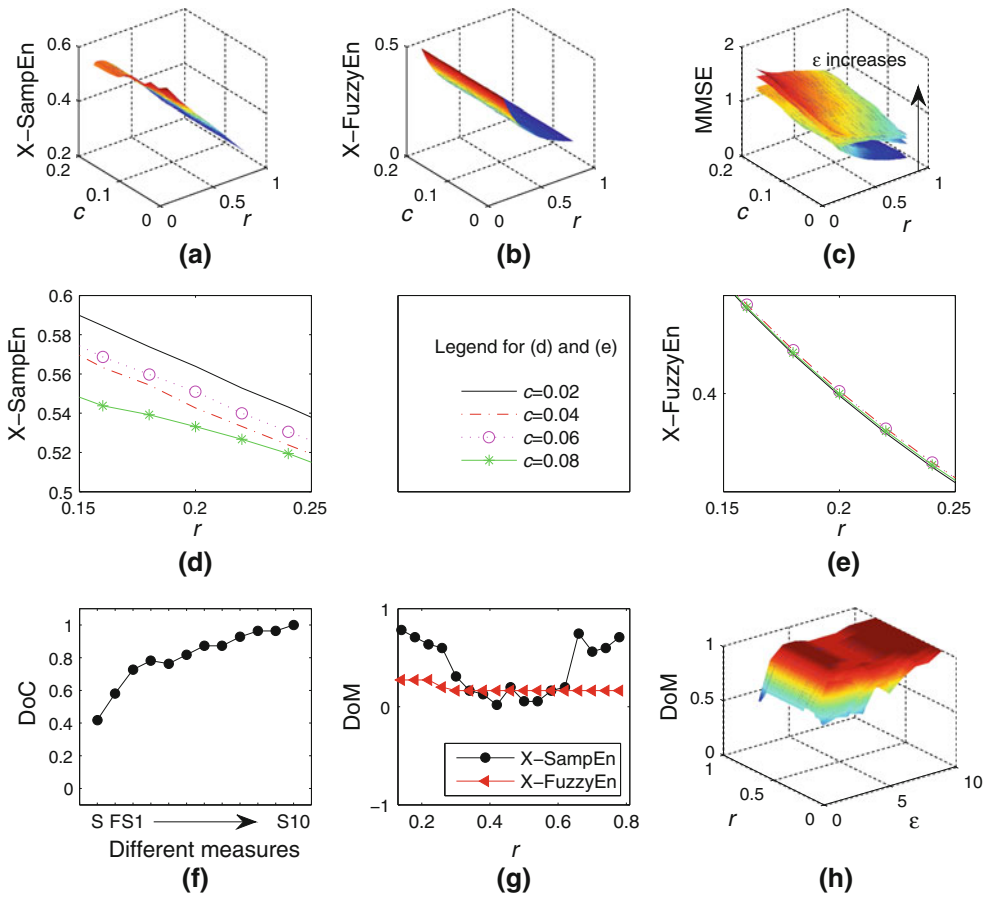

Fig. 4 Simulation results for coupled Rössler systems (M4). **a** A 3D-plot of [*r*, *c*, X-SampEn]. **b** A 3D-plot of [*r*, *c*, X-FuzzyEn]. **c** A sliced-3D-plot of [*r*, *c*, MMSE]. **d** The projection of X-SampEn versus *r*. **e** The projection of X-FuzzyEn versus *r*. **f** DoC values of X-SampEn, X-FuzzyEn and MMSE. **g** DoM values of X-SampEn and X-FuzzyEn. **h** DoM values of MMSE. X-SampEn (S), X-FuzzyEn (F) and MMSE of all 10 scales (S1 → S10) are shown from left to right in (**f**). The *curves* are plotted every other point in (**g**)

(consecutive R–R intervals within an ECG sequence) and IBI series (consecutive inter-beat intervals within a simultaneously recorded respiration sequence) from each subject were used. To avoid the potential influence of spikes introduced by premature ventricular contractions or distortion in signal recordings [22], we applied an anomalous-intervals-removing process [20] priori to their calculation. In addition, the same to simulated models, we chose the first 500 points from RRI and IBI series for the calculation of X-SampEn and X-FuzzyEn, and the first 5,000 points for MMSE. For rigor, the corresponding randomized surrogate series were also produced (by randomly reordering).

Figure 5 shows the overall performances on the original and randomized bivariate signals (RRI and IBI series) of them. The MMSE values at larger scales for the randomized surrogates are lower than that for the original bivariate signals, confirming a complex temporal structure within RRI and IBI series. X-SampEn and X-FuzzyEn for the healthy elderly are severely overlapped with those for the healthy young, while the separation between the MMSE

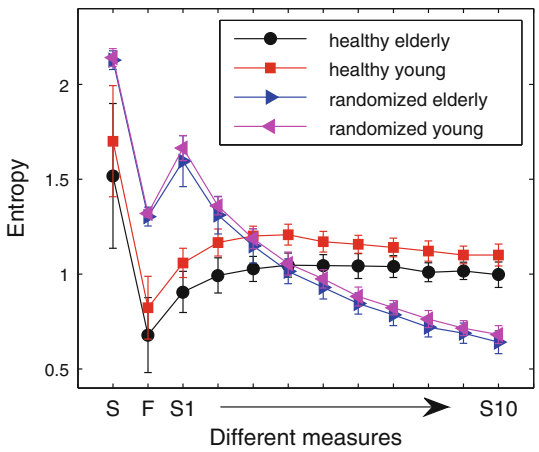

Fig. 5 An application to cardiorespiratory coupling analysis. The *curves* represent an average of 10 subjects and *error bars* the standard deviation (SD)

curves is higher, especially at medium and larger scales. MMSE decrease significantly, whereas larger X-SampEn and X-FuzzyEn values showed in healthy elderly.

4 Discussion

It is an open problem to adequately determine interactions between bivariate physiological systems where their coupling is not known a priori. Synchronization provides an insight into the underlying interaction mechanisms. There are probably 100 or even more measures have been developed for testing it (the readers can refer to studies of Ansari-Asl et al. [4], Kreuz et al. [17] and Dauwels et al. [10] for a review). Among them, most measures test only the local time synchronicity, e.g., generalized synchrony [27, 28], phase synchrony [26], event synchrony [24], etc. But it is also believed that a tight coupling can cause predictable pattern architectures, which provides as the basis of pattern synchronization (PS). PS focuses on the similarity of patterns in the whole time range among different channels of signals. It can be tested using a variety of entropy-based measures. These measures are fully data-driven; hence suitable for direct analysis of nonlinear and non-stationary systems. However, their calculation requires three pre-defined parameters, among which the threshold value r is proved to be the most influencing factor [8, 18, 19, 21]. The empirical values might give incorrect results when applied to the complex physiological systems. Although Xie et al. [31] published a comparative study and concluded that X-FuzzyEn performed better than X-SampEn in terms of degree of monotonicity and robustness against noise. But they used a fixed r (0.15) when simulating. According to our most recent study [18], crossing-over also could not be avoided even using X-FuzzyEn when r varied. Thus, it is uncertain whether the results of Xie et al's study would be the same or not when adopting another r. Also there is currently no publications about how r influences MMSE.

Therefore, we tried to gain an insight into the various behaviors of different PS measures using different model systems in this study. We used coupled broadband noise model (M1), coupled MIX(p) processes (M2), coupled Hénon maps (M3) and coupled Rössler systems (M4) for our testing. These models have been widely employed to represent a wide range of signal dynamics encountered in physiological recordings [4, 17, 19]. Thereinto, the first two systems have a stochastic nature and the last two have a chaotic nature. We tested three measures—cross sample entropy (X-SampEn), cross fuzzy entropy (X-FuzzyEn) and multivariate multiscale entropy (MMSE)—in this work and defined two geometry-based criteria to quantify their performances (consistency and distinguishability).

Our results demonstrate that single scale analysis (X-SampEn and X-FuzzyEn) may only be acceptable on coupled stochastic systems (M1 and M2). This is reminiscent of multiscale entropy for complexity analysis of univariate time-series [9]. Stochastic systems fundamentally reveal fewer structures and thus their pattern similarity could be well exhibited in single scale. Besides, X-SampEn fails to make a distinction between coupled systems with higher amount of low-frequency trend (M2, with very low DoM values). We have reported a similar phenomenon before [18]. In this case, X-FuzzyEn performs better than X-SampEn. This may be explained by the removing of a local average when calculating X-FuzzyEn [31, 32], which makes it less sensitive to the low-frequency trend. In addition, X-SampEn is less robust with large fluctuations in different trials. It reminds us that our calculation procedure will make the results more credible than that just from one random realization as was done in [31]. It is worth noting that for acceptable results when applying them, a suitably selected r is required. Since it seems no regular behavior showed in our results, a retrospective analysis of pragmatically chosen one value which most reliably yields valuable information should be one solution although it needs large amount of calculation.

However, MMSE works well on both coupled stochastic systems (M1 and M2) and coupled chaotic systems (M3 and M4) without much consideration on the selection of r, especially at medium or larger scales. For MMSE at smaller scales, it may fail because it has a SampEn nature at these scales [1, 2]. This again addressed that complex dynamics need multiple scales to reveal their intrinsic structures. Besides, with higher amount of low-frequency trend (M2), MMSE at larger scales also fails. Since mainly low-frequency components are present at larger scales, their influence to MMSE needs to be considered. It might be advisable to apply de-trend algorithms first.

By comparison, the analysis in multiply scales overwhelms the substitution of fuzzy membership function for the Heaviside function (one improvement in consistency, see [7, 32] for a review) when complex dynamics is dominant. However, one problem in MMSE is the distinct decrease of the length at larger scales due to the coarse-graining procedure. To capture scales more robustly, many efforts are now under their way [3, 13].

Overall, we argue that MMSE is relatively superior to X-SampEn and X-FuzzyEn in terms of consistency and distinguishability. Our final analysis on cardiorespiratory PS convincing it, which shows low separation of the latter two between different age groups and an opposing conclusion as to MMSE. But it does not mean that the latter two measures are totally not desirable. For several coupled systems (stochastic-featured), they could work with meticulously selected r. However, it seems difficult to make a rule for its selection. According to our simulation, we tried to make some recommendations (see Table 2), not just for the selection of r but also their suitable applications. It should also be noted that PS is definitely not the only way to test the dynamical interactions. Other measures

Table 2 Recommendations of the selection of the threshold value r and suitable application for three pattern synchronization measures

Application	Measures	Selection of r[a]	Others
Stochastic systems	X-SampEn	Retrospective analysis	De-trend first if necessary. Most physiological systems are nonlinear in nature, yet MMSE is recommended. Robust approach for capturing scales is further required for improvement.
	X-FuzzyEn	Ditto for accurate, or empirically 0.15–0.25	
	MMSE	0.15–0.8, better 0.2–0.4	
Nonlinear complex chaotic systems	X-SampEn	Not recommended	
	X-FuzzyEn		
	MMSE	0.15–0.8, better 0.2–0.4	

[a] Note that all numbers below are for normalized time-series

such as normalized mutual information are also capable. However, we are not trying to show their differences; they just capture different aspects of the interactions. They could be complementary, but further studies are required.

To summarize, this study evaluates the consistency and distinguishability of three PS measures—X-SampEn, X-FuzzyEn and MMSE by four simulation models and performs one validation on real cardiorespiratory coupling analysis. Only with meticulously selected threshold value r, the former two measures can work for coupled stochastic systems. It is not recommended to apply them for analyzing the intrinsically complex physiological systems. MMSE is showed to be catered for both with relatively higher consistency and distinguishability, which is thus highly recommended.

Acknowledgments We would like to thank Prof. Danilo P. Mandic and Dr. Mosabber U. Ahmed from Imperial College for fruitful discussions. Also we thank Miss. Xinning Liu from School of Foreign Languages and Literature, Shandong University for her help in polishing this paper. We are also grateful to the anonymous reviewers for their insightful comments which helped us improving the quality of this paper.

This work is supported by the Graduate Independent Innovation Foundation of Shandong University (GIIFSDU, yzc12082), the National Natural Science Foundation of China (61201049), the Excellent Young Scientist Awarded Foundation of Shandong Province (BS2012DX019) and the Independent Innovation Foundation of Shandong University (IIFSDU, 2011GN069).

References

1. Ahmed MU, Mandic DP (2011) Multivariate multiscale entropy: a tool for complexity analysis of multichannel data. Phys Rev E 84(6):061918
2. Ahmed MU, Mandic DP (2012) Multivariate Multiscale Entropy Analysis. IEEE Signal Process Lett 19(2):91–94
3. Ahmed MU, Rehman N, Looney D, Rutkowski TM, Mandic DP (2012) Dynamical complexity of human responses: a multivariate data-adaptive framework. Bull Pol Ac: Tech 60(3):433–445
4. Ansari-Asl K, Senhadji L, Bellanger JJ, Wendling F (2006) Quantitative evaluation of linear and nonlinear methods characterizing interdependencies between brain signals. Phys Rev E 74(3 Pt 1):031916
5. Bartsch RP, Schumann AY, Kantelhardt JW, Penzel T, Ivanov P (2012) Phase transitions in physiologic coupling. Proc Nat Acad Sci USA 109(26):10181–10186
6. Castiglioni P, Di Rienzo M (2008) How the threshold "R" influences approximate entropy analysis of heart-rate variability. In: Murray A (ed) Computers in Cardiology. IEEE, Bologne, pp 561–564
7. Chen W, Zhuang J, Yu W, Wang Z (2009) Measuring complexity using FuzzyEn, ApEn, and SampEn. Med Eng Phys 31(1):61–68
8. Chon K, Scully CG, Lu S (2009) Approximate entropy for all signals. IEEE Eng Med Biol Mag 28(6):18–23
9. Costa M, Goldberger AL, Peng CK (2002) Multiscale entropy analysis of complex physiologic time series. Phys Rev Lett 89(6):068102
10. Dauwels J, Vialatte F, Musha T, Cichocki A (2010) A comparative study of synchrony measures for the early diagnosis of Alzheimer's disease based on EEG. NeuroImage 49(1):668–693
11. Goldberger AL (1996) Non-linear dynamics for clinicians: chaos theory, fractals, and complexity at the bedside. Lancet 347(9011):1312–1314
12. Goldberger AL, Amaral LA, Glass L, Hausdorff JM, Ivanov PC, Mark RG, Mietus JE, Moody GB, Peng CK, Stanley HE (2000) PhysioBank, PhysioToolkit, and PhysioNet: components of a new research resource for complex physiologic signals. Circulation 101(23):E215–E220
13. Hu M, Liang H (2012) Adaptive multiscale entropy analysis of multivariate neural data. IEEE Trans Biomed Eng 59(1):12–15
14. Hu Z, Shi P (2006) Interregional functional connectivity via pattern synchrony. In: 9th International Conference on Control, Automation, Robotics and Vision, Singapore, IEEE, pp 1–6
15. Iyengar N, Peng CK, Morin R, Goldberger AL, Lipsitz LA (1996) Age-related alterations in the fractal scaling of cardiac interbeat interval dynamics. Am J Physiol Heart Circ Physiol 271(4): R1078–R1084
16. Kennel MB, Brown R, Abarbanel HDI (1992) Determining embedding dimension for phase-space reconstruction using a geometrical construction. Phys Rev A 45(6):3403–3411
17. Kreuz T, Mormann F, Andrzejak RG, Kraskov A, Lehnertz K, Grassberger P (2007) Measuring synchronization in coupled model systems: a comparison of different approaches. Physica D 225(1):29–42
18. Li P, Liu CY, Wang XP, Li B, Che WB, Liu CC (2012) Cross-sample entropy and cross-fuzzy entropy for testing pattern synchrony: how results vary with different threshold value r. In: Long M (ed) IFMBE Proceeding World Congress on medical physics and biomedical engineering. Springer, Beijing, pp 485–488
19. Liu CY, Liu CC, Shao P, Li LP, Sun X, Wang XP, Liu F (2011) Comparison of different threshold values r for approximate entropy: application to investigate the heart rate variability between heart failure and healthy control groups. Physiol Meas 32(2):167–180
20. Liu CY, Li LP, Zhao LN, Zheng DC, Li P, Liu CC (2012) A combination method of improved impulse rejection filter and template matching for identification of anomalous intervals in RR sequences. J Med Biol Eng 32(4):245–250
21. Lu S, Chen X, Kanters JK, Solomon IC, Chon KH (2008) Automatic selection of the threshold value r for approximate entropy. IEEE Trans Biomed Eng 55(8):1966–1972
22. Molina-Pico A, Cuesta-Frau D, Aboy M, Crespo C, Miro-Martinez P, Oltra-Crespo S (2011) Comparative study of approximate entropy and sample entropy robustness to spikes. Artif Intell Med 53(2):97–106

23. Pincus SM (1991) Approximate entropy as a measure of system complexity. Proc Nat Acad Sci USA 88(6):2297–2301
24. Quian Quiroga R, Kreuz T, Grassberger P (2002) Event synchronization: a simple and fast method to measure synchronicity and time delay patterns. Phys Rev E 66(4):041904
25. Richman JS, Moorman JR (2000) Physiological time-series analysis using approximate entropy and sample entropy. Am J Physiol Heart Circ Physiol 278(6):H2039–H2049
26. Rosenblum MG, Pikovsky AS, Kurths J (1996) Phase Synchronization of Chaotic Oscillators. Phys Rev Lett 76(11):1804–1807
27. Rulkov NF, Sushchik MM, Tsimring LS, Abarbanel HDI (1995) Generalized synchronization of chaos in directionally coupled chaotic systems. Phys Rev E 51(2):980–994
28. Schiff SJ, So P, Chang T, Burke RE, Sauer T (1996) Detecting dynamical interdependence and generalized synchrony through mutual prediction in a neural ensemble. Phys Rev E 54(6):6708–6724
29. Vakorin VA, Ross B, Krakovska O, Bardouille T, Cheyne D, McIntosh AR (2010) Complexity analysis of source activity underlying the neuromagnetic somatosensory steady-state response. NeuroImage 51(1):83–90
30. Wagner CD, Persson PB (1998) Chaos in the cardiovascular system: an update. Cardiovasc Res 40(2):257–264
31. Xie H, Guo J, Zheng Y (2010) A comparative study of pattern synchronization detection between neural signals using different cross-entropy measures. Biol Cybern 102(2):123–135
32. Xie H, Zheng Y, Guo J, Chen X (2010) Cross-fuzzy entropy: a new method to test pattern synchrony of bivariate time series. Inform Sciences 180(9):1715–1724
33. Zhang T, Yang Z, Coote JH (2007) Cross-sample entropy statistic as a measure of complexity and regularity of renal sympathetic nerve activity in the rat. Exp Physiol 92(4):659–669